Journal of Alloys and Compounds 525 (2012) 154–158

Contents lists available at SciVerse ScienceDirect

Journal of Alloys and Compounds

journal homepage: www.elsevier.com/locate/jallcom

Microwave-assisted one-pot synthesis of water-soluble rare-earth doped fluoride luminescent nanoparticles with tunable colors

Cong-Cong Mi[a], Zhen-huang Tian[a], Bao-fu Han[a], Chuan-bin Mao[b], Shu-kun Xu[a,*]

[a] *Department of Chemistry, Northeastern University, Shenyang 110819, PR China*
[b] *Department of Chemistry & Biochemistry, Stephenson Life Sciences Research Center, University of Oklahoma, 101 Stephenson Parkway, Norman, OK 73019, USA*

ARTICLE INFO

Article history:
Received 15 November 2011
Received in revised form 9 February 2012
Accepted 13 February 2012
Available online xxx

Keywords:
Microwave-assisted synthesis
Multicolor luminescence
Nanomaterials

ABSTRACT

Polyethyleneimine (PEI) functionalized multicolor luminescent LaF_3 nanoparticles were synthesized via a novel microwave-assisted method, which can achieve fast and uniform heating under eco-friendly and energy efficient conditions. The as-prepared nanoparticles possess a pure hexagonal structure with an average size of about 12 nm. When doped with different ions (Tb^{3+} and Eu^{3+}), the morphology and structure of the nanoparticles were not changed, whereas the optical properties varied with doped ions and their molar ratio, and as a result emission of four different colors (green, yellow, orange and red) were achieved by simply switching the types of doping ions (Eu^{3+} versus $Tb^{3}+$) and the molar ratio of the two doping ions.

1. Introduction

Rare earth doped luminescent nanomaterials possess many advantages, such as narrow emission peak, long fluorescence lifetime, high photochemical stability, and large stokes shift [1]. Moreover, it is easy to achieve multicolor emission under a single excitation by changing doped rare earth ions or matrix [2]. In recent years, synthesis and applications of rare-earth doped nanomaterials have attracted wide interest [3–5]. Rare earth doped nanomaterials have broad applications in protein and DNA assays [6], bio-labeling [7], optical imaging [8], magnetic resonance imaging (MRI) [9] and clinical diagnostics. Over the last few decades, various solution phase routes, including precipitation [10], thermal decomposition [11], polyol-mediated process [12], micro-emulsion [13], sol–gel [14], hydrothermal [15] and two phase method [16] have been applied for the preparation of rare earth doped nanoparticles. Most recently, Tang et al. reported the preparation of $GdVO_4$:Eu^{3+} nanocrystals with different morphologies through hydrothermal method and investigated the effects of annealing temperature and rare earth ions doping concentration on the luminescence intensity [17]. Chen et al. synthesized Pr^{3+} and Yb^{3+} ions co-doped down- and up-conversion transparent oxyfluoride, during which the maximum quantum efficiency from Pr^{3+}:$^3P_0$ to Yb^{3+}:$^2F_{5/2}$ was 153% [18]. Zheng et al. synthesized sphere-like $CaWO_4$:Mo/Eu,Tb microspheres, they found that proper doping concentration of Mo extended excitation range of the microspheres [19]. Kuznik et al. investigated fluorescent properties of gadolinium oxide powders doped with different rare earth ions (Er^{3+}, Tb^{3+}, Dy^{3+}). They found that singly doped Er^{3+} sample gave stronger luminescence signals and others showed significantly larger decay lifetimes [20].

Here, we describe a novel microwave-assisted solvothermal approach for the fast and rapid preparation of small spherical single phase LaF_3 nanoparticles. As a kind of green synthetic method, in recent years, microwave-assisted preparation has been developed rapidly. In a microwave system, heating arises from either dipole rotation or ion migration induced by the microwave field, which is different from radiation, conduction and convection of traditional heating method [21]. Consequently, compared with the conventional methods, microwave irradiation shows several advantages, including even and selective heating, shortened reaction time, less side effects, smaller and narrower particle size, and higher yield [22]. Due to the unique heating model, microwave-assisted method has received more and more attention and been widely used in the preparation and extraction of chemical, biological and medicinal materials. It has been employed to exploit new materials. As a new heating source, microwave irradiation has been successfully used in a number of chemical approaches to produce many types of nanoparticles, such as metal [23], II–VI group semiconductors [24], oxides [25], vanadium metal-organic frameworks [26], fluoride [27], phosphates [28,29], and even for the grafting of poly(9,90-n-dihexylfluorene) (PDHF) onto flat and nanopatterned crosslinked photopolymer [30].

Rare earth fluoride has very low phonon energy, and can directly stimulate the f–f transition of rare earth ions [31]. Therefore, research on the synthesis and application of rare earth fluoride is of

---

[*] Corresponding author. Tel.: +86 24 83681343.
E-mail address: xushukun46@126.com (S.-k. Xu).

0925-8388/$ – see front matter © 2012 Elsevier B.V. All rights reserved.
doi:10.1016/j.jallcom.2012.02.095

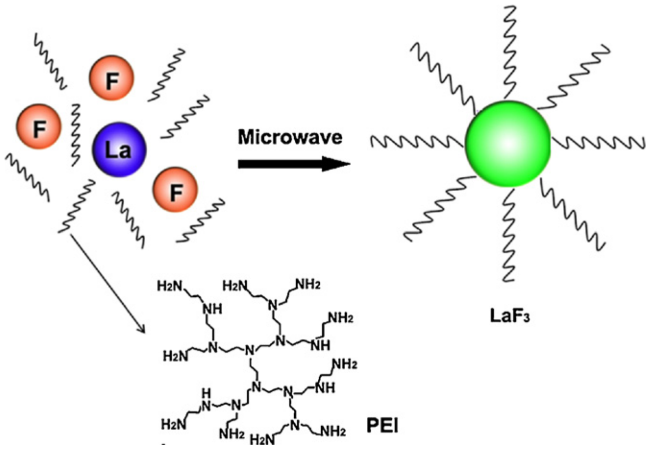

Scheme 1. Diagram illustrating the formation of PEI modified LaF_3 nanoparticles.

great significance. Among them, the Eu^{3+} and Tb^{3+} ions doped inorganic nanoparticles possess strong red and green luminescence, respectively, and their applications in biological and medical field have received much attention [32,33]. There are few reports on the synthesis of rare earth doped fluoride materials, such as CeF_3 and $NaYF_4$ by microwave hydrothermal method [34,35] and synthesis of LaF_3 superfine powder from $La(CH_3COO)_3$ and NH_4F by microwave heating method [36]. In this work, one-pot synthesis and modification of LaF_3 nanoparticles via microwave solvothermal method was reported for the first time and PEI was used for surface functionalization of the nanoparticles during preparation. By this novel one-pot method, a four-color system was obtained through controlling the doping amount of Eu^{3+} and Tb^{3+} ions in the LaF_3 matrix. X-ray diffraction (XRD), transmission electron microscopy (TEM), photoluminescence (PL) and Fourier transform infrared spectroscopy (FT-IR) were used to characterize the as-synthesized nanoparticles.

The diagram for the formation of LaF_3 nanoparticles was shown in Scheme 1. During the experiment, a mixture of $Ln(NO_3)_3{\cdot}nH_2O$ and NaF were dispersed in ethylene glycol. With the elevating of temperature, rare earth ions gradually reacted with F^- ions to form the tiny particles. After kept at the set temperature for a certain time, the tiny nanoparticles grew up to single phase nanocrystals, and could emit various luminescence colors such as green, yellow, orange and red when different rare earth ions were doped. In addition, PEI was used to cover the surface of the nanoparticles to improve their water-solubility, so finally the amino functionalized hydrophilic nanoparticles were obtained.

2. Experimental

The LaF_3 nanoparticles were synthesized with a MD6C-4H Microwave Digestion System (Ying An Mei Cheng Company, Beijing China). Reagents used in the experiment, such as ethylene glycol, sodium fluoride (NaF), lanthanum chloride ($LaCl_3$), cerium chloride heptahydrate ($CeCl_3{\cdot}7H_2O$), terbium nitrate ($Tb(NO_3)_3{\cdot}6H_2O$), europium oxide (Eu_2O_3), were purchased from Sinopharm Chemical Reagent Co., Ltd. (Shanghai, China). All of the reagents were of analytical grade and used as received without further purification. PEI10000 (50%) was purchased from Sigma (U.S.A.). Europium nitrate ($Eu(NO_3)_3$) was obtained by dissolving and evaporating europium oxide in nitric acid. Triple distilled water was used through out the experiment.

Typically, for the synthesis of LaF_3:Ce,Tb nanoparticles, $La(NO_3)_3{\cdot}6H_2O$ (0.4179 g), $CeCl_3{\cdot}7H_2O$ (0.0559 g), $Tb(NO_3)_3{\cdot}6H_2O$ (0.1019 g) and NaF (0.1890 g) were mixed in ethylene glycol (20 mL). The mixture was thoroughly stirred and sonicated to form a homogeneous solution, then transferred to an autoclave, sealed and kept at 120 °C for 30 min. After reaction, the autoclave was allowed to cool naturally to room temperature and then opened. The final products were collected by centrifugation at 8500 rpm for 5 min, washed with ethanol and water to remove any remnants, and dried at 60 °C for 1 h. Preparation of the nanoparticles modified with PEI was nearly same as the procedure mentioned above, except that 500 μL PEI was used during the synthesis.

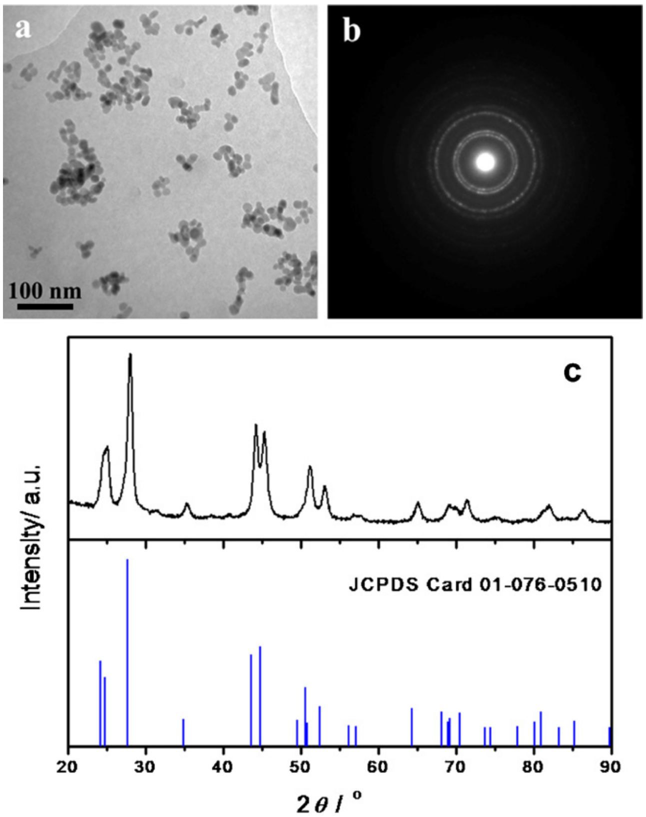

Fig. 1. TEM (a), SAED (b) and XRD (c) patterns of the as-prepared LaF_3:Ce,Tb nanoparticles.

Preparation of LaF_3:Eu nanoparticles was similar to that of LaF_3:Ce,Tb. First, $La(NO_3)_3{\cdot}6H_2O$ (0.3900 g) was mixed with $Eu(NO_3)_3$ (2.25 mL, 0.2 mol·L^{-1}) and NaF (0.1890 g) in ethylene glycol. The solution was also stirred to be homogeneous and treated at 150 °C for 30 min. The subsequent steps to obtain the products was carried out just as procedure mentioned above for the preparation of LaF_3:Ce,Tb nanoparticles.

3. Results and discussion

3.1. Morphology and nanostructure of the nanoparticles

The morphology and electron diffraction patterns of the as-prepared nanoparticles was characterized on a TECNAI G2 20 transmission electron microscope (TEM, FEI Ltd., USA), with an accelerating voltage of 200 kV. Fig. 1a and b show the TEM image and selected area electron diffraction (SAED) pattern of as-synthesized LaF_3:Ce,Tb nanoparticles. The nanoparticles are uniform in shape with an average diameter of 12 nm. Size distribution of the nanoparticles showed that the average size was 15 nm,

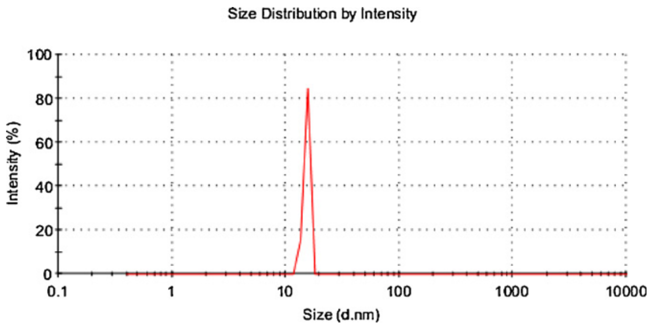

Fig. 2. Size distribution the as-prepared LaF_3:Ce,Tb nanoparticles.

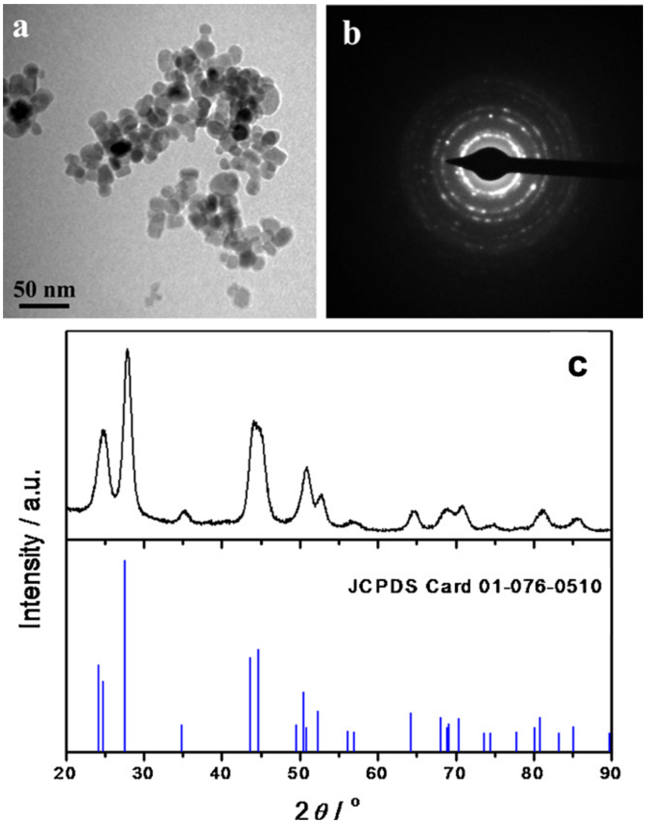

Fig. 3. TEM (a), SAED (b) and XRD (c) patterns of the as-prepared LaF_3:Eu nanoparticles.

which was basically consistent with the TEM (Fig. 2). SAED pattern in Fig. 1b shows a series of clear diffraction rings demonstrating that the nanoparticles are highly crystalline.

The crystal phase of the as-prepared products was identified by an X'Pert Pro diffractometer (Panalytical Co., Holland) using Cu Kα radiation ($\lambda = 1.5406$ Å), at a scan rate of 8° min^{-1}. Fig. 1c shows the XRD pattern of the as-synthesized LaF_3:Ce,Tb nanoparticles and the standard pattern. It is clear that all the diffraction peaks can be readily indexed to the hexagonal LaF_3 (JCPDS card 01-076-0510). The results showed that the obtained nanoparticles remained phase-pure LaF_3 after Ce^{3+} and Tb^{3+} were doped at the concentrations up to 10% and 15%, respectively, suggesting that the Ce^{3+} and Tb^{3+} ions have been effectively doped into the crystal lattices of the hexagonal LaF_3 phase. According to the XRD data, we could calculate the size of as-synthesized LaF_3:Ce,Tb nanoparticles through Debye–Scherrer equation ($D = K\lambda/\beta\cos\theta$, where D is the diameter of the particle, K is normally equal to 0.89 and λ is the wavelength of X-ray radiation, β is FWHM of diffraction peak and θ is the Bragg diffraction angle). Based on the calculation, the average size of the prepared LaF_3:Ce,Tb nanoparticles was 12 nm, which is consistent with the result of TEM image shown in Fig. 1a.

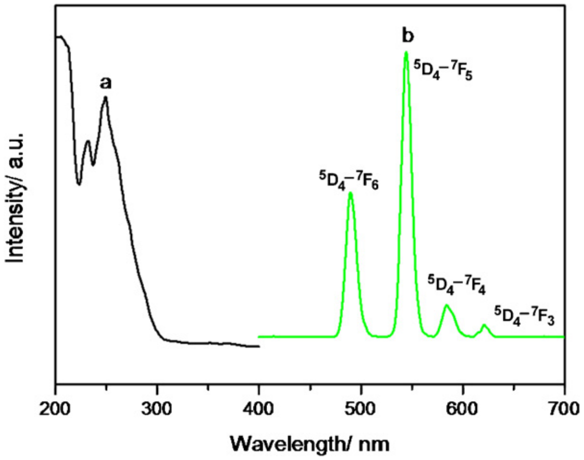

Fig. 4. The excitation (a) and emission (b) spectra of as-prepared LaF_3:Ce,Tb nanoparticles.

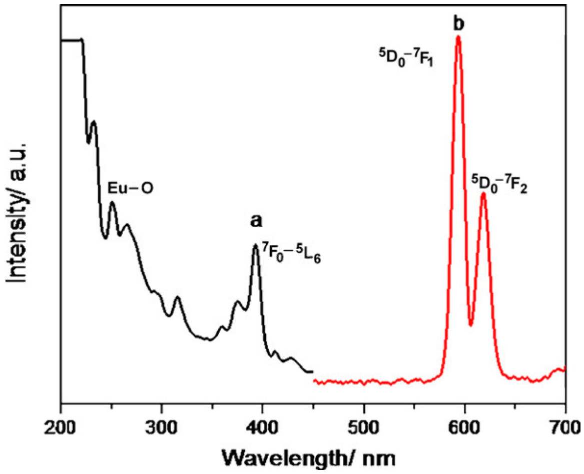

Fig. 5. The excitation (a) and emission (b) spectra of as-prepared LaF_3:Eu nanoparticles.

As we all known, the doped ions will directly affect the optical properties of materials so it is easy to achieve multi-color emission under a single excitation by changing doped rare earth ions. Here, by using Eu^{3+} ions to replace Ce^{3+} and Tb^{3+} ions, the LaF_3:Eu nanoparticles were synthesized under the same method. Morphology, structure and optical properties of the Eu^{3+} doped nanoparticles were also obtained from TEM, XRD and PL, respectively. Fig. 3a is the TEM image of as-prepared LaF_3:Eu nanoparticles. It is clear that all of the nanoparticles are nearly spherical, and the average size of the nanoparticles is about 13 nm. The diffraction rings in Fig. 3b shows that the nanoparticles are highly crystalline. Fig. 3c represents the XRD pattern of the as-prepared LaF_3:Eu nanoparticles and the standard pattern. It shows that Eu^{3+} doped LaF_3 nanoparticles were still phase-pure and possessed a hexagonal structure. Meanwhile, after calculation using the Debye–Scherrer equation, the size of the as-prepared LaF_3:Eu nanoparticles was 13 nm. From the TEM images and XRD patterns of the as-synthesized Ce^{3+}/Tb^{3+} and Eu^{3+} doped nanoparticles,

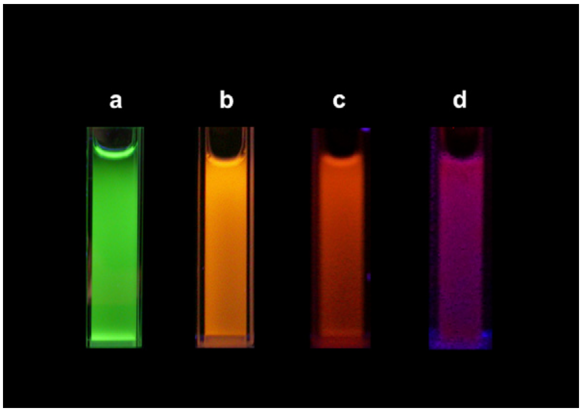

Fig. 6. Multicolor luminescent photograph of LaF_3 nanoparticles doped with (a) 15 mol%Tb, (b) 25 mol% Tb, 5 mol% Eu, (c) 15 mol% Tb, 5 mol% Eu and (d) 30 mol% Eu.

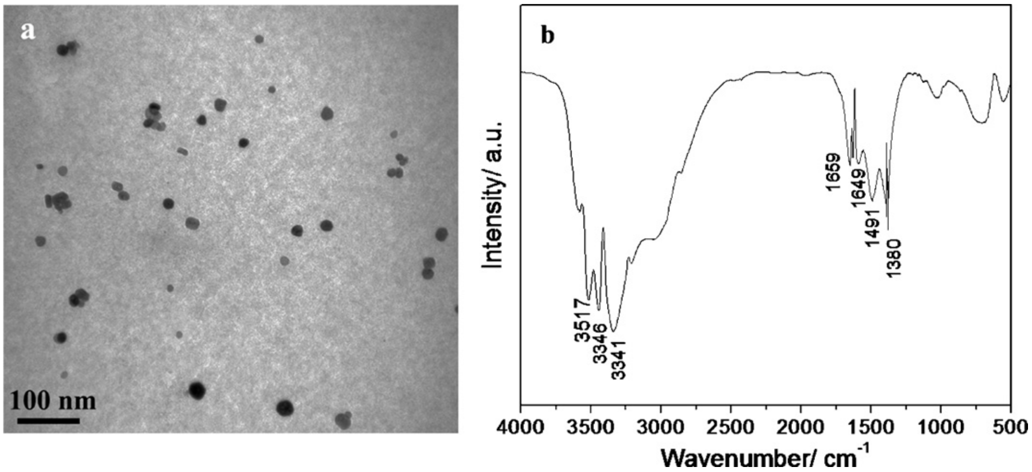

Fig. 7. TEM image (a) and IR spectrum (b) of LaF_3:Ce,Tb nanoparticles one-pot synthesized and modified with PEI.

it can be concluded that there is neither obvious change in the particle size, nor distinction in the crystal structure of the products when different rare earth ions were doped.

3.2. Optical properties of the nanoparticles

Photoluminescence excitation and emission spectra of the nanoparticles were acquired on a LS-55 luminescence spectrometer (Perkin-Elmer Co., USA). Digital photos were taken by a Nikon camera from the samples dispersed in deionized water at a concentration of 0.05 wt%. Fig. 4 shows the photoluminescence spectra of the as-synthesized LaF_3:Ce,Tb nanoparticles at room temperature. In the excitation spectrum (Fig. 4a), the narrow peak at 252 nm was contributed by 4f–5d transition of Ce^{3+} ions [37]. The emission spectrum located from 450 to 650 nm was mainly composed of four peaks (Fig. 4b), which were separately corresponding to the f-f transitions of Tb^{3+} from the excited $^5D_4$ levels to the ^7F_J ($J = 6, 5, 4, 3$) levels [38,39]. After calculated, the quantum yield of the synthesized nanoparticles was 60%, luminescence lifetime was 5.1 ms.

The excitation and emission spectra of as-synthesized LaF_3:Eu nanocrystals (monitored at 593 nm and 392 nm, respectively) are shown in Fig. 5. The major excitation peak at 392 nm in Fig. 5a is corresponding to the $^7F_0$–$^5L_6$ transition of Eu^{3+} ions. The weak peak at 249 nm can be assigned to the charge transfer band between Eu^{3+} and the surrounding oxygen anions, indicating that there is a small amount of oxygen atoms existing within the crystal [40]. Fig. 5b is the emission spectrum of LaF_3:Eu nanocrystals monitored at 392 nm. The typical emission peaks at 593 and 615 nm were attributed to $^5D_0$–$^7F_1$ and $^5D_0$–$^7F_2$ transition of Eu^{3+} ions, respectively [32,41]. Through measurement, the luminescence lifetime of the LaF_3:Eu nanocrystals was 5.2 ms.

Recently, many studies have been performed for the fabrication of multicolor nanoparticles, due to their important role in multimodal bio-imaging [42]. Various colors can be achieved by the adjustment of doped rare earth ions and their concentrations. During this experiment, four colors phosphors were obtained by doping Ce^{3+}/Tb^{3+} and Eu^{3+} ions into the crystal lattices of the hexagonal LaF_3 phase and controlling their relative amounts. The multicolor luminescent photograph of Ce^{3+}/Tb^{3+} and Eu^{3+} ions doped LaF_3 nanoparticles with different concentrations taken at 252 nm excitation is shown in Fig. 6. It is clearly shown that when doped with Tb^{3+}, the synthesized LaF_3 nanoparticles showed bright green luminescence. The luminescence was changed to red when Eu^{3+} was doped for the replacement of Tb^{3+} ions. Meanwhile, nanoparticles co-doped with both Tb^{3+} and Eu^{3+} ions exhibit yellow and orange emission due to the presence of two dopants with different molar ratios.

3.3. One-pot modification of the nanoparticles

For the future biological application as a probe, the luminescent nanoparticles usually need to be modified with amino or carboxyl groups. Here, the synthesized nanoparticles were directly modified with PEI during the synthetic procedure. TEM image and IR spectrum of the modified nanoparticles were presented in Fig. 7. PEI is a long chain polymer, which can be adsorbed on the surface of nanoparticles during preparation. It plays an important role as a modifier. In addition, the steric hindrance from long chain of PEI molecules can effectively inhibit the aggregation of nanoparticles. After modification, the size of the nanoparticles was increased slightly, reaching to 15–25 nm (Fig. 7a). Fig. 7b shows the IR spectrum of PEI modified nanoparticles. Peaks from 3517–3341 cm^{-1} and 1659–1380 cm^{-1} are attributed to the stretching and bending vibration of NH_2 groups, respectively, suggesting successful coating of nanoparticles by PEI.

4. Conclusions

In summary, we have demonstrated a novel method for the preparation of Ce^{3+}/Tb^{3+} and Eu^{3+} ions doped LaF_3 nanoparticles. The as-prepared nanoparticles were absolute hexagonal crystals, with an average size of about 12 nm. A four-color system was obtained through doping Ce^{3+}/Tb^{3+} and Eu^{3+} ions into the crystal lattices of hexagonal phase LaF_3 and adjusting their doping concentrations. This system can not only be made water-soluble and bearing amino groups for conjugation with antibodies, but also be excited by one light to emit different visible colors, enabling its future applications in biological labeling and imaging.

Acknowledgments

This work was funded by the National Science Foundation of China (Grant No. 20875011), and the support from Northeastern University on PhD students. CBM would like to thank the financial support from the US National Science Foundation (DMR-0847758, CBET-0854414, and CBET-0854465), National Institutes of Health (R21EB009909-01A1, R03AR056848-01, and R01HL092526-01A2), and Oklahoma Center for the Advancement of Science and Technology (HR11-006#7823).

References

[1] S.V. Eliseevaa, J.C.G. Bünzli, Chem. Soc. Rev. 39 (2010) 189.
[2] D. Zhao, S.J. Seo, B.S. Bae, Adv. Mater. 19 (2007) 3473.
[3] J. Zhang, Y.H. Wang, Y. Wen, F. Zhang, B.T. Liu, J. Alloys Compd. 509 (2011) 4649.
[4] N. Niu, P.P. Yang, Y. Wang, W.X. Wang, F. He, S.L. Gai, D. Wang, J. Alloys Compd. 509 (2011) 3096.
[5] K. Binnemans, Chem. Rev. 109 (2009) 4283.
[6] J.L. Worlinsky, S. Basu, J. Phys. Chem. B 113 (2009) 865.
[7] W.H. Di, J. Li, N. Shirahata, Y. Sakka, M.G. Willinger, N. Pinna, Nanoscale 3 (2011) 1263.
[8] S.V. Eliseeva, J.C.G. Bünzli, New J. Chem. 35 (2011) 1165.
[9] K. Hickmann, K. Kömpe, A. Hepp, M. Haase, Small 4 (2008) 2136.
[10] Z.Y. Wang, L.M. Wang, Z.Q. Li, Mater. Lett. 65 (2011) 3516.
[11] J.C. Boyer, J. Gagnon, L.A. Cuccia, A.C. John, Chem. Mater. 19 (2007) 3358.
[12] Z.L. Wang, Z.W. Quan, P.Y. Jia, C.K. Lin, Y. Luo, Y. Chen, J. Fang, W. Zhou, C.J.O'Connor, J. Lin, Chem. Mater. 18 (2006) 2030.
[13] G.F. Wang, W.P. Qin, J.S. Zhang, Y. Wang, C.Y. Cao, L.L. Wang, G.D. Wei, P.F. Zhu, R.J. Kim, J. Phys. Chem. C 112 (2008) 12161.
[14] A. Patra, C.S. Friend, R. Kapoor, P.N. Prasad, Chem. Mater. 15 (2003) 3650.
[15] K.L. Wong, G.L. Law, M.B. Murphy, P.A. Tanner, W.T. Wong, P.K.S. Lam, M.H.W. Lam, Inorg. Chem. 47 (2008) 5190.
[16] N.N. Zhao, W. Nie, J. Mao, M.Q. Yang, D.P. Wang, Y.H. Lin, Y.D. Fan, Z.L. Zhao, H. Wei, X.L. Ji, Small 6 (2010) 2558.
[17] S. Tang, M.L. Huang, J.L. Wang, F.D. Yu, G.L. Shang, J.H. Wu, J. Alloys Compd. 513 (2012) 474.
[18] Q.J. Chen, W.J. Zhang, X.Y. Huang, G.P. Dong, M.Y. Peng, Q.Y. Zhang, J. Alloys Compd. 513 (2012) 139.
[19] Y.H. Zheng, Y.J. Huang, M. Yang, N. Guo, H. Qiao, Y.C. Jia, H.P. You, J. Lumin. 132 (2012) 362.
[20] W. Kuznik, M.G. Brik, I. Cieslik, A. Majchrowski, L. Jaroszewicz, N.S. AlZayed, A.M. El-Naggar, I. Sildos, S. Lange, V. Kiisk, I.V. Kityk, J. Alloys Compd. 511 (2012) 221.
[21] E. Caponetti, D.C. Martino, M. Leone, L. Pedone, M.L. Saladino, V. Vetri, J. Colloid Interface Sci. 304 (2006) 413.
[22] H.Q. Wang, T. Nann, ACS Nano 3 (2009) 3804.
[23] S. Horikoshi, H. Abe, T. Sumi, K. Torigoe, H. Sakai, N. Serpone, M. Abe, Nanoscale 3 (2011) 1697.
[24] D.W. Ayele, H.M. Chen, W.N. Su, C.J. Pan, L.Y. Chen, H.L. Chou, J.H. Cheng, B.J. Hwang, J.F. Lee, Eur. Chem. J. 17 (2011) 57237.
[25] Z.H. Ai, K.J. Deng, Q.F. Wan, L.Z. Zhang, S. Lee, J. Phys. Chem. C 114 (2010) 6237.
[26] A. Centrone, T. Harada, S. Speakman, T.A. Hatton, Small 6 (2010) 1598.
[27] M. Pang, D.P. Liu, Y.Q. Lei, S.Y. Song, J. Feng, W.Q. Fan, H.J. Zhang, Inorg. Chem. 50 (2011) 5327.
[28] G. Buhler, C. Feldmann, Angew. Chem. 118 (2006) 4982.
[29] L. Ma, L.M. Xu, W.X. Chen, Z.D. Xu, Mater. Lett. 63 (2009) 1635.
[30] W. Moran, S.B. Jhaveri, K.R. Carter, Small 4 (2008) 1176.
[31] L.J. Charbonnière, J.L. Rehspringer, R. Ziessel, Y. Zimmermann, New J. Chem. 32 (2008) 1055.
[32] P.P. Wang, B. Bai, L.J. Huang, S. Hu, J. Zhuang, X. Wang, Nanoscale 3 (2011) 2529.
[33] E. Beaurepaire, V. Buissette, M.P. Sauviat, D. Giaume, K. Lahlil, A. Mercuri, D. Casanova, A. Huignard, J.L. Martin, T. Gacoin, J.P. Boilot, A. Alexandrou, Nano Lett. 4 (2004) 2079.
[34] L. Ma, W.X. Chen, X.Y. Xu, L.M. Xu, X.M. Ning, Mater. Lett. 64 (2010) 1559.
[35] J. Olesiak-Banska, M. Nyk, D. Kaczmarek, K. Matczyszyn, K. Pawlik, M. Samoc, Opt. Mater. 33 (2011) 1419.
[36] Y.F. Wu, Y.W. Tian, Y.S. Han, Y.C. Zhai, C.Z. Wang, Trans. Nonferrous Met. Soc. China 14 (2004) 738.
[37] F. Li, M. Wang, C.C. Mi, K.Y. Yi, S.K. Xu, J. Alloys Compd. 486 (2009) L37.
[38] P. Ghosh, A. Kar, A. Patra, J. Phys. Chem. C 114 (2010) 715.
[39] P. Ghosh, A. Kar, A. Patra, Nanoscale 2 (2010) 1196.
[40] Y.J. Sun, H.J. Liu, X. Wang, X.G. Kong, H. Zhang, Chem. Mater. 18 (2006) 2726.
[41] P. Ghosh, A. Patra, J. Phys. Chem. C 112 (2008) 19283.
[42] J. Zhou, Y. Sun, X.X. Du, L.Q. Xiong, H. Hu, F.Y. Li, Biomaterials 31 (2010) 3287.